Civil Engineering Infrastructures Journal, 49(1): 111 – 126, June 2016
Print ISSN: 2322-2093; Online ISSN: 2423-6691
DOI: 10.7508/ceij.2016.01.008

Seismic Bearing Capacity of Strip Footings on Pile-Stabilized Slopes

Haghbin, M.[1*] and Ghazavi, M.[2]

[1] Assistant Professor, Department of Civil Engineering, Islamshahr Branch, Islamic Azad University, Islamshahr, Iran.
[2] Professor, Department of Civil Engineering, KN Toosi University of Technology, Tehran, Iran.

Received: 06 Jun. 2015; Revised: 10 Dec. 2015; Accepted: 23 Dec. 2015

ABSTRACT: This paper develops an analytical method to calculate seismic bearing capacity of a strip footing, which is located on a slope reinforced with rows of pile. The resistance of passive pile is determined based on normal and shear stress of the soil around the pile, which is then compared to other analytical methods. This comparison indicates an acceptable agreement. The variants of the study include location of pile rows, location of footing with respect to the slope crest, foundation depth, and horizontal seismic coefficient. The footing seismic bearing capacity is calculated based on seismic slope stability with limit analysis method (yield acceleration coefficient of reinforced slope with pile row) as well as soil stability beneath the footing by means of virtual retaining wall method. The main objective is to determine and establish the relation between various parameters and seismic bearing capacities of the footing, and to find the best location of the pile row that gives the best improvement in the footing seismic bearing capacity. Results indicate that stabilizing the earth slope with rows of piles has a significant effect on the improvement of seismic bearing capacity of the footing. In addition, the results of the present method are compared with those, reported by others, to demonstrate a reasonable agreement.

Keywords: Analytical Method, Footing, Footing Bearing Capacity, Pile, Seismic, Slope, Yield Acceleration.

INTRODUCTION

There could be many cases where footings are constructed on sloping ground or adjacent to a slope crest, such as footings for bridge abutments on sloping embankments. In such cases (when the footings are placed on sloping ground), their bearing capacity is reduced based, on their locations and with respect to the slope, slope height, and soil type. As a result, it is not likely to see shallow foundations, employed in such situations.

The use of retaining piles to support an active earth slope has been regarded as a slope reinforcement method in the last few decades. The lateral force, acting on each passive pile may be obtained in an approximate manner by multiplying the resisting force per unit width of the pile via center-to-center spacing of the piles in a row. However, arching between adjacent

* Corresponding author E-mail: haghbin@iiau.ac.ir

piles should be taken into consideration so that the force acting on the piles is determined more accurately.

Several analytical methods were suggested to determine the effects of pile on slope stability (Auslio et al., 2001; Hassiotist and Chameau, 1997; Munawir et al., 2013; Liu and Geo, 2015; Mehmetl, 2009; Ren-Ping, 2009; Azzam, 2010; Mofidi et al., 2014; Farzaneh et al., 2009). Xinpo et al. (2010) studied seismic stability of the slope, reinforced with a row of pile. For so doing he made use of a limit analysis method in which the seismic displacement and yield acceleration of the reinforced slope were determined. Several studies have been conducted in order to find out the best position of stabilizing pile row within a slope (Hassiotist and Chameau, 1997; Ito et al., 1975). Besides, numerical methods were used to determine the safety factor of the reinforced slope with pile row (Wei and Cheng, 2009).

Mostafa and Sawwaf (2005) reported experimental results of bearing capacity of the strip footing on the slope, reinforced with a pile row and sheet-pile. Also numerical studies were reported about bearing capacity of footing on the pile-stabilized slopes as well (Munawir et al., 2013).

Scientific investigations use analytical, numerical, or experimental approaches. While experimental methods are often costly and time-consuming, they can be used to verify the results from other methods with the conventional methods to solve problems being the analytical ones. In many cases, we cannot find analytical solutions for practical problems, in which case the governing equations must be solved numerically in spite of approximate approach. In addition, problem's solutions in numerical methods must be validated experimentally or analytically by the works of others from the literature.

Although previous researches have not presented any analytical method to determine the bearing capacity of footing on pile stabilized slope, they have given numerical and experimental ones (Mostafa and Sawwaf, 2005; Munawir et al., 2013). As a 3D method is time-consuming, especially for a dynamic analysis, parametric studies with such a method get complicated. Moreover, seismic bearing capacity of footing on the pile stabilized slope cannot be simply determined with experimental and numerical methods. The story is, however, different with the analytical method which takes less time.

Most of previous studies on pile-stabilized slopes have only considered slope stability, whereas the improvement of load-carrying characteristics of shallow footings, supported on the pile stabilized slopes has rarely given any proper attention. In this paper, an analytical method is developed to determine the seismic bearing capacity of strip footing on the pile-reinforced slope. The bearing capacity is calculated based on seismic slope stability by means of limit analysis method, as well as seismic stability of soil beneath the footing via both limit analysis and virtual retaining wall methods. The minimum seismic bearing capacity between the two methods is selected as seismic bearing capacity of the footing. The varied parameters, investigated in this study, include location of pile rows, location of footing relative to the slope crest, foundation depth, and horizontal seismic coefficient, mainly to determine and establish a connection of some sort between these parameters and the seismic bearing capacity of the footing, and to find out the best location of the piles row which gives the best improvement in the footing seismic bearing capacity.

ANALYSIS METHOD

The seismic bearing capacity of a footing on pile-reinforced slope was studied analytically. It is calculated based on soil stability beneath the footing, determined from both virtual retaining wall method and seismic slope stability. Seismic stability of slopes, reinforced with rows of pile, is analyzed using kinematic theory of limit analysis within the framework of the pseudo-static approach. As a matter of fact, the present study employs supper bound limit analysis method. The first step to achieve this goal is to determine pile resistance against soil movement, as seismic slope stability and soil stability beneath the footing depend on the lateral resistance of the passive pile in a slope. It is assumed here that soil failure obeys Mohr-Coulomb yield criterion.

Ito and Matsui (1975) presented a method to calculate lateral pressures on piles located passively in a plastically-deforming ground, considering the soil squeeze between the piles (Figure 1). They considered two types of plastic states in the ground, surrounding the passive pile. One state, referred to as the theory of plastic deformation, satisfies Mohr-Coulomb yield criterion while the other state, known as the theory of plastic flow, considers the ground as a visco-plastic solid material. In fact, this method calculates the total force, applied on piles, along with the soil between the piles, with the force on the soil between the piles, subtracted from the total force. Afterwards, the force, applied on each pile, is determined (Figure 1)

Ito and Matsui's method (1975) has a limited range of assumptions, valid only for rigid piles, one pile row, and fixed piles in stable layer. The method is unable to consider the effect of earth slope and seismic loading. The proposed method, however, ameliorates these limiting assumptions when determining passive pile resistance. Previous studies confirmed the results from their method so long as its assumptions were similar to the field data. Therefore, Ito and Matsui method has been used to show the validity of the one, proposed in this paper.

When the piles spacing in a row is minimum (ratio of spacing to diameter of piles is equal to 2.5), lateral resistance of the passive pile at various depths is determined, using Eq. (1) (Figure 2).

$$p_u = (\eta K_p^2 \gamma z + \eta K_{pc}^2 c)b + (\xi K \gamma z \tan\delta)b \quad (1)$$

in which γ: is soil density, c: is soil cohesion, z: is depth, ξ: is shape factor, b: is pile diameter, η: is shape factor, K_p: is soil passive pressure coefficient, K_{pc}: is passive coefficient of soil cohesion, δ: is friction between soil and pile, and K: is coefficient of lateral earth pressure (ratio of horizontal to vertical effective stress, $1-\sin\phi$). Both K_p and K_{pc} are determined with Coulomb method.

$$K_p = \frac{\cos^2(\phi+\theta-\psi)}{\cos^2\theta\cos^2\psi\cos(\theta-\delta-\psi)\left[1-\sqrt{\frac{\sin(\phi+\delta)\sin(\phi+\beta-\psi)}{\cos(\theta-\delta-\psi)\cos(\theta-\beta)}}\right]^2} \quad (2)$$

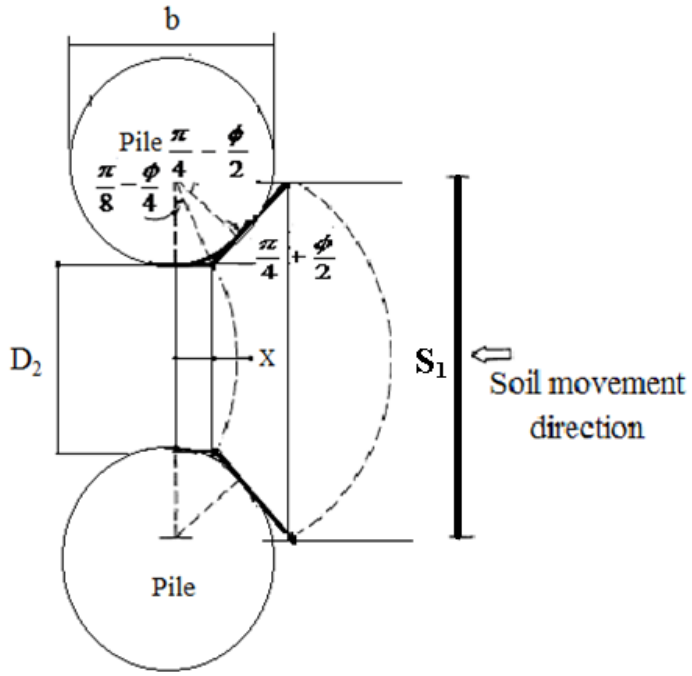

Fig. 1. Plastic deformation of ground around stabilizing piles (Ito et al., 1975)

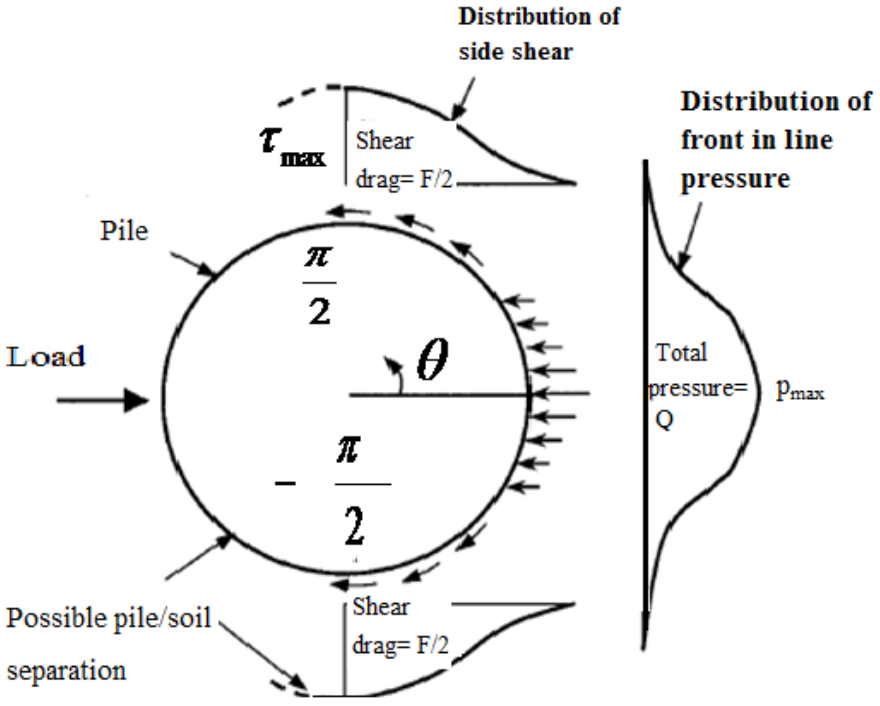

Fig. 2. Distribution of frontal soil resistance and side shear resistance in passive pile (Hassiotist et al., 1997)

where, $\psi = \tan^{-1}\frac{k_h}{1-k_v}$, k_h: is horizontal seismic coefficient, k_v: is vertical seismic coefficient, θ: is pile angle with vertical direction, β: is slope angle, and ϕ: is internal friction of soil.

$$K_{pc} = 2\sqrt{K_p(1+\frac{c_w}{c})} \quad (3)$$

where $c_w = 0.5c$ when c <50 kPa, and c_w=25 kPa when c > 50 kPa. It is noteworthy that the first and second terms in Eq. (1) indicate normal resistance while the third one indicates shear resistance of soil around the pile.

The present study determines the lateral resistance of the passive pile by simulating the piles as wall and adding shear resistance of the soil surrounding them. In addition, plastic deformation of soil between the piles in a row affects their lateral resistance and power of passive coefficients. The latter represents the effect from combining soil plastic deformation between piles in a row and pile resistance, and varies for different spacing of piles in a row, causing the power of K_p and K_{pc} become equal to 2 (Eq. (1)) when the ratio of piles' spacing in a row to pile diameter becomes minimum (S_1/b = 2.5). Also, when S_1/b = 8, the power of passive coefficients is equal to 1 and the plastic deformation of the soil between piles does not affect lateral resistance of the pile. Similarly, the effect of pile spacing in a row on soil plastic deformation between piles was obtained by Ito and Matsui (1975) along with Wei and Cheng (2009) using the computer software, called FLAC3D.

The effect of seismic coefficient and slope condition on lateral pile resistance is included in the soil passive pressure coefficient. In seismic slope stability method, the pile resistance is calculated in sliding and stable layers, and pile lateral resistance equals minimum resistance in these layers. It is notable that Eq. (1) was used to calculate active pile resistance against external load in cohesion-less soil.

In general, the capabilities of the proposed method are outlined as follows:

- The pile fixity in stable layer has been taken into account; therefore, the lateral resistance of flexible piles can be incorporated.
- Spacing between the piles in rows can be taken into consideration.
- The effect of ground slope as well as seismic effects has been incorporated.
- The variation of bending moment and shear force along the pile can be calculated in sliding and stable layers.

The following section depicts how the proposed method is developed so that it could determine the seismic bearing capacity of a footing, constructed on a pile-reinforced slope.

Seismic Bearing Capacity, Based on Stability of the Soil beneath Footing (Virtual Retaining Wall Method)

As shown in Figure 3, this method assumes an imaginary retaining wall, which passes through the footing edge, close to the slope crest. As seen in Figure 3, this virtual wall's height is defined as H_1 in order to calculate bearing capacity of the footing on the pile-reinforced slope. This method was reported to be able to determine bearing capacity of the footing on flat ground (without pile). As observed, the wall tolerates active force (Pa) due to the footing loading and the soil beneath the footing. The surrounding soil on the left of the wall is passive and exerts passive force P_p on the wall. The values of P_a and P_p are computed with Coulomb lateral earth pressure method. The active force P_a is:

$$P_a = q_{ult} K_a H_1 \cos\delta + \frac{1}{2} K_a \gamma (1 - k_v) H_1^2 \cos\delta - cK_{ac} H_1 \cos\delta \quad (4)$$

where B: is width of foundation, $H_1 = B\tan\eta_{ae}$, q_{ult}: is footing bearing capacity, c: is soil cohesion, η_{ae}: is angle of active wedge with horizontal direction (Figure 3), δ: is friction angle between soil and wall, K_a: is active lateral earth pressure, and K_{ac}: is active coefficient of soil cohesion in Coulomb method:

$$K_{ac} = 2\sqrt{K_a(1 + \frac{c_w}{c'})} \quad (5)$$

The passive force from soil weight and pile force within a reinforced slope with pile is determined by equalizing the passive zone forces. This gives:

$$P_p = \cos\delta \frac{\frac{W_1}{\cot(\eta_{pe} + \phi)} + F_p + V_B}{\frac{\sin\delta}{\cot(\phi + \eta_{pe})} + \cos\delta} \quad (6)$$

where η_{pe}: is angle of passive wedge with horizontal direction (Figure 3) , W_1: is weight of passive wedge, F_p: is resistance of pile in passive zone, and V_B: is shear force at the hinged pile head.

The slope angle (β) affects W_1 in Eq. (6), where the pile resistance (F_p) is determined according to Eq. (1) in which the pile length is equal to length of the pile in the passive zone. If the total length of the pile is embedded in the passive zone, the pile resistance is measured with total length of the pile in the virtual retaining wall method. It is noted that passive force, obtained from foundation depth and soil cohesion is:

$$P_{p1} = (K_p(1 - k_v)\gamma D H_1 + K_{pc} c H_1)\cos\delta \quad (7)$$

where D: is footing embedded depth.

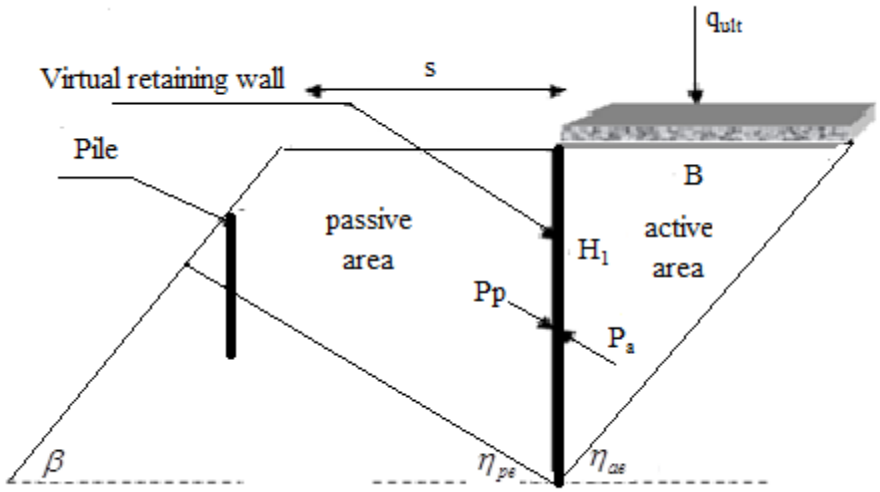

Fig. 3. Failure mechanism of soil beneath footing (virtual retaining wall method)

The seismic bearing capacity of the footing is determined by equalizing active and passive forces, as shown in Figure 3.

$$q_{ult} = cN_c + \gamma DN_q + 0.5\gamma BN_\gamma + \frac{P_p}{K_a B \tan\eta_{ae}} \quad (8)$$

where $N_c = \frac{K_{pc} + K_{ac}}{K_a}$,

$N_\gamma = -\tan\eta_{ae}(1-k_v)$, $N_q = \frac{K_p}{K_a}(1-k_v)$.

The seismic effect on the footing bearing capacity is incorporated in $\gamma, \eta_{ae}, \eta_{pe}, K_p$, K_{pc}, K_{ac}, K_a and P_p. It also affects the lateral pile resistance through F_{p1}. In fact, seismic condition has an influence on failure mechanism of the soil beneath the footing and also, active and passive forces. The above algorithm is written in MATLAB to determine q_{ult}.

Bearing Capacity, Based on Seismic Slope Stability (Yield Acceleration Coefficient of Slope)

In this section, the seismic bearing capacity of footing located on slope is determined based on seismic slope stability analysis. A program is then written in MATLAB, using slope stability analysis. The seismic stability of the slopes reinforced with pile rows is analyzed using upper bound limit analysis within the framework of pseudo-static approach. In the present study, a homogeneous and isotropic soil slope, reinforced with pile rows is taken into consideration. Based on limit analysis method, the soil is assumed to deform plastically, based on the normality rule associated with Mohr-Coulomb yield condition. Of all various failure mechanisms of slope, the rotational one has been found to be the most adverse for earth slopes; therefore, the rotational log-spiral collapse mechanism, examined earlier by Chen (1975), is chosen herein. The geometry of the sliding surface is described by the following log-spiral equation (Figure 4):

$$r = r_0 e^{(\theta-\theta_0)\frac{\tan(\phi)}{FS}} \quad (9)$$

where r_0: is radius of the log spiral with respect to angle θ_0, *FS*: is safety factor, and θ_0: is shown in Figure 4.

The failing soil rotates as a rigid body around the rotation center with angular velocity ω. The slope geometry is defined by height *H*, and angles α and β which are also demonstrated in Figure 4.

The kinematic method of limit analysis states that a slope will collapse if the rate of work done by external loads, body forces, and surcharge force exceed the energy dissipation rate for any assumed admissible rupture surface. The rate of external work due to the soil weight and surcharge force takes the form:

$$\begin{aligned} \dot{W}_1 &= \gamma r_0^3 \dot{\omega}(f_1 - f_2 - f_3 - f_4) \\ &+ qL_1\dot{\omega}\left[r_0 \cos(\theta_0 + \alpha) - \frac{L_1}{2}\right] \\ &+ sL_1\dot{\omega}r_0 \sin(\theta_0 + \alpha) \end{aligned} \quad (10)$$

where q: is vertical surcharge, s: is horizontal surcharge, L_1: is length of surcharge effect and the functions $f_1 - f_4$ depend on the angles θ_0, θ_h, ϕ, β and β', calculating the area of failure surface by multiplying vertical displacement. Expressions for $f_1 - f_4$ are indicated in the APPENDIX and can be found in several works (Auslio et al., 2001; Xinpo et al., 2010).

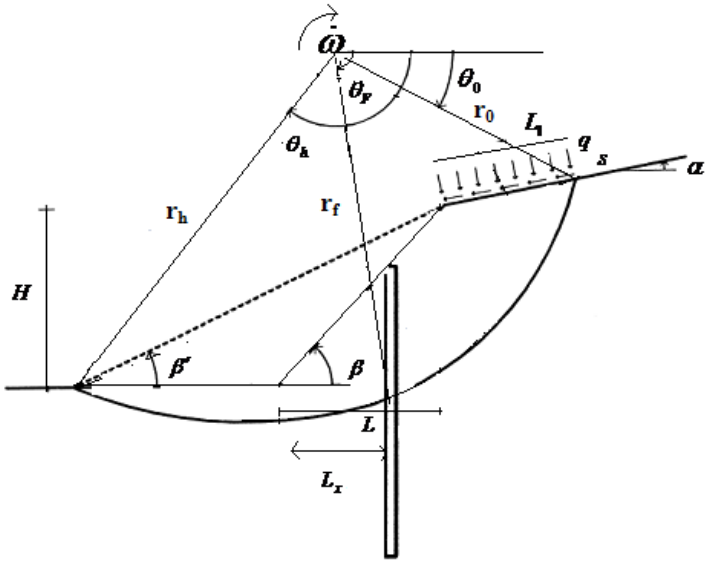

Fig. 4. Slope failure mechanism (Xinpo et al., 2010)

Once the slope is subjected to earthquake loading, the rate of the inertial force should be considered in the energy balance equation. An earthquake affects a potential sliding mass by the force, acting horizontally at the center of gravity which is determined as the product of a seismic coefficient k_h, and the weight of the potential sliding mass. In the present study, the vertical acceleration and the impacts of soil resistance alterations due to earthquake loading are not taken into account, while a uniform distribution of lateral earthquake force is assumed. The rate of external work due to earthquake force is written as:

$$\dot{W}_2 = k_h \gamma r_0^3 \dot{\omega}(f_5 - f_6 - f_7 - f_8) \tag{11}$$

where expressions for $f_5 - f_8$ are indicated in the Appendix. $f_5 - f_8$ calculate the weight of failure surface, multiplying the horizontal displacement.

The rate of energy dissipation caused by soil cohesion is:

$$\dot{D}_1 = c r_0^2 \dot{\omega} f_9 \tag{12}$$

where, f_9: is introduced in the Appendix and f_9 calculates length of sliding surface.

To account for the presence of the passive piles, the lateral resistance is calculated with the proposed method, explained before. It is notable that the pile resistance is equal to the minimum resistance in sliding and stable layer. The rate of energy dissipation, caused by the passive piles is:

$$\dot{D}_2 = F_p \sin(\theta_F) r_F \dot{\omega} \tag{13}$$

where F_p: is the resistance of passive pile, r_F: is the distance of F_p around the rotation center, and the angle θ_F: is the location of the passive piles.

The upper bound solution for the coefficient of the slope's yield acceleration can be presented if the rate of internal energy dissipation is equalized with the external rate of work.

$$\dot{W}_1 + \dot{W}_2 = \dot{D}_1 + \dot{D}_2 \tag{14}$$

Substituting Eqs. (10-13) into Eq. (14) results in:

$$k_y = \frac{cr_0^2 f_9 + F_p \sin(\theta_F) r_F - qL(r_0 \cos(\theta_0 + \alpha) - \frac{L}{2}) - sLr_0 \sin(\theta_0 + \alpha) - \gamma r_0^3 (f_1 - f_2 - f_3 - f_4)}{\gamma r_0^3 (f_5 - f_6 - f_7 - f_8)} \quad (15)$$

where k_y: is the upper-bound solution of the acceleration coefficient for the log-spiral rupture surface.

The critical seismic coefficient is determined by minimizing k_y with respect to θ_0, θ_h and β'. It means to initially take the first derivatives of k_y and then equate them as zero.

$$\frac{\partial k_y}{\partial \theta_0} = 0, \ \frac{\partial k_y}{\partial \theta_h} = 0, \ \frac{\partial k_y}{\partial \beta'} = 0 \quad (16)$$

Eq. (16) can be solved knowing the force F_p, and the critical values of θ_0, θ_h and β'. Putting values of θ_0, θ_h and β' into Eq. (15), the least upper-bound value for the yield acceleration coefficient k_c, is calculated. In the present study, k_c is calculated with the program, written in MATLAB.

In the written program, various collapse mechanisms (log spiral) are examined with changing $\theta_0, \theta_h, \beta'$ to find the collapse mechanism giving the minimum critical acceleration coefficient. The yield acceleration coefficient is determined for various surcharges (q) in this method and the seismic bearing capacity for various locations of the pile in the slope is determined, based on acceleration coefficient of the specific area. Therefore, the seismic bearing capacity is equal to the surcharge the slope can tolerate when the yield acceleration coefficient becomes equal to the acceleration coefficient of the specific area in question.

The minimum seismic bearing capacity between two methods (seismic slope stability method and virtual retaining wall method), described above, is regarded as the ultimate bearing capacity of the strip footing, located on the pile-reinforced slope.

RESULTS AND DISCUSSIONS

Comparison of the Proposed Method with Ito and Matsui's Method

Figure 5 compares the results of the proposed method and those by Ito and Matsui (1975) to determine lateral resistance of passive pile, where the same assumptions by them are also considered and the results are identical in many items. Previous studies indicate that results, obtained by Ito and Matsui agree with the field data, proving the validity of the proposed method.

Comparison of Slope Yield Acceleration Coefficient, Calculated Using the Proposed Method with Other Method

The proposed method is used here to determine passive pile resistance for further calculation of the yield acceleration coefficient of slope through limit analysis method. Figure 6 illustrates the features of this model. Results have been compared to the method, presented Xinpo et al. (2010). Table 1 shows the safety factors and the yield acceleration coefficient of slope once with the pile, located 12.2 m from the slope toe, and once without it. The proposed method and Xinpo's vary in computation of passive pile resistance. Xinpo et al. (2010) applied IM method to calculate lateral resistance of passive pile and limit the analysis method to calculate yield acceleration coefficient of the slope with the same assumptions made in IM method. Results indicate that yield acceleration coefficient of the slope with the pile row, which employs the proposed method is close

to those from Xinpo's with the slight difference, just related to slope's effect on pile resistance. The Safety Factor (FS) for reinforced slope with pile row in the proposed method is also relatively the same as Xinpo's.

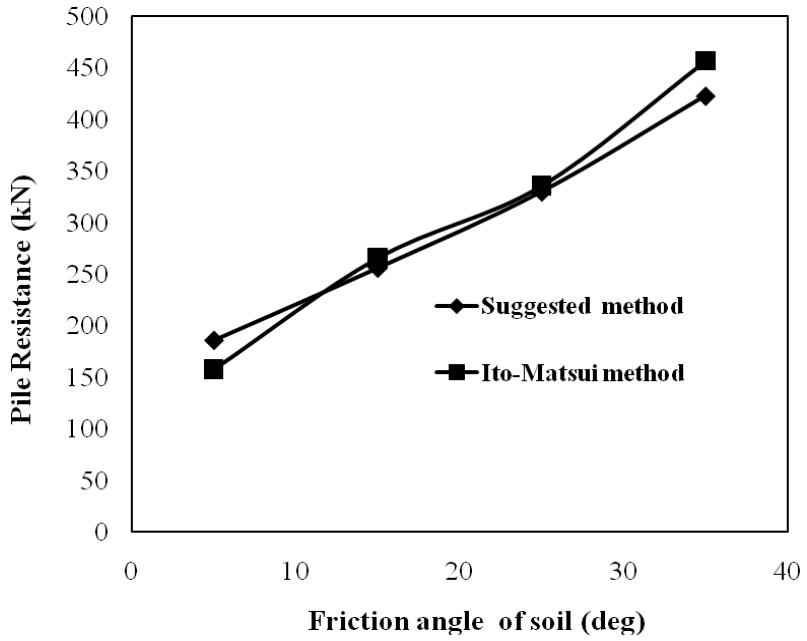

Fig. 5. Comparison between the proposed method to determine lateral resistance of passive pile and Ito and Matsui's method (1975) for various soil friction angles (S_1/b = 2.5, pile length in sliding layer = 4 m)

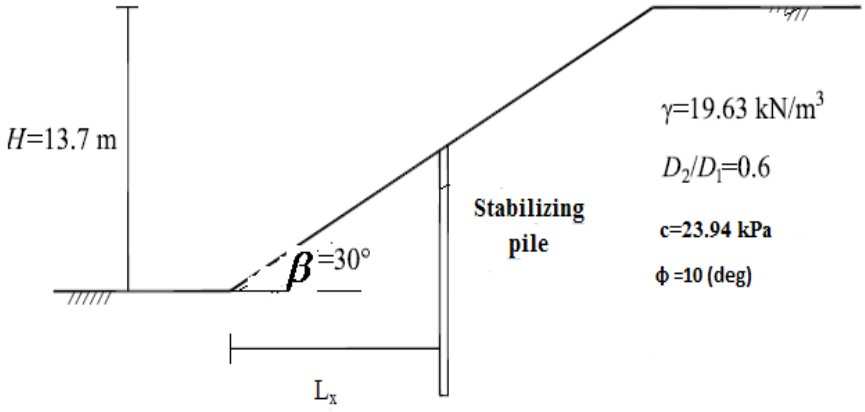

Fig. 6. Model properties in Xinpo's research

Table 1. Comparison of the proposed method with Xinpo's research

Condition of Slope	c (kPa)	φ (deg)	FS			k_c		
			(Bishop's Method)	(Xinpo Method)	(Proposed Method)	(Newmark Method)	(Xinpo Method)	(Proposed Method)
Without Piles	23.94	10	1.12	1.11	1.18	0.053	0.061	0.07
With Piles	23.94	10	---	2.45	2.55	----	0.25	0.29

Comparison of the Proposed Method to Determine Seismic Bearing Capacity of the Footing on Unreinforced Slope with other Methods

Table 2 compares seismic footing bearing capacity on unreinforced slope by means of the proposed method with those, calculated by Meyerhof (1963), Hansen (1970), Saran et al. (1989), and Choudhury and Rao (2006). Model properties are as follows: slope angle = 30 degrees, *D/B* = 1 degree, and soil friction angle = 35 degrees with the soil, being cohesion-less. As seen in Table 2, bearing capacity of the footing on the unreinforced slope is calculated when k_h = 0, 0.1, and 0.2 and k_v = 0. Results show that the proposed method is close to that of Choudhury and Rao (2006). Although the results from the proposed method are not close to others, the computed bearing capacity of the footing lies in between. Table 2 demonstrates that the highest value of seismic bearing capacity belongs to Meyerhof method, and the least to Hansen.

Parametric Studies

This section studies the effects of pile rows' locations, footing's location relative to the slope crest, foundation depth, and horizontal seismic coefficient on seismic bearing capacity of the footing located on the slope, reinforced with pile rows. Two methods are employed to calculate the seismic bearing capacity, namely seismic slope stability and virtual retaining wall methods. It is noteworthy that in case of a pile row, positioned far from the passive zone, the presence of piles that use the virtual retaining wall method does not affect the footing seismic bearing capacity (Figure 3); however, the slope's stability is under the influence of the pile, present at various parts of the slope. In seismic slope stability method, pile resistance and footing bearing capacity depend on the shape of rupture surface and pile length. Seismic bearing capacity is then determined somehow in between these two methods (slope stability and virtual retaining wall methods), depending on various parameters to be discussed.

In this section the properties, assumed, include: soil friction angle (ϕ) = 30°, soil density (γ) = $19.63\frac{kN}{m^3}$, cohesion of soil = 2 kPa, slope height (*H*) = 13.7 m, and slope angle (β) = 30°. For piles, it is assumed that the diameter (b) = 1 m, pile head is free, pile length (L_p/b) = 10, 20 and center to center spacing of piles (S_1) = 2.5 m. The strip footing width (*B*) = 2 m, foundation depth (*D/B*) = 0, 0.5, ratio of distance of foundation from the slope crest to foundation width (*S/B*) = 0, 1, horizontal seismic coefficient (k_h) = 0.1, 0.4, and L_x/L = ratio of pile location from slope toe to slope length.

Table 2. Comparison of the proposed method to determine seismic bearing capacity of the footing on unreinforced slope with other methods (values in kPa)

k_h	Proposed Method	Hansen (1970)	Meyerhof (1963)	Choudhury and Rao (2006)	Saran et al. (1989)
0	527	300	760	520	730
0.1	408	220	612	390	480
0.2	294	160	413	250	401

One of the main objectives of the present paper is to find out the best location of pile row in slopes that result in maximum footing seismic bearing capacity. Therefore, maximum seismic bearing capacity in the results and discussions above refer to maximum footing seismic bearing capacity, obtained by altering pile location in slope.

Effect of foundation location with respect to slope crest (S)

Figure 7a demonstrates the impact of foundation distance with respect to the slope crest (S) and the pile location in the slope on the footing seismic bearing capacity (L_p/b = 20, D/B = 0). It shows that the pile, which result in maximum footing seismic bearing capacity, varies depending on its location; and this maximum capacity increases as a consequence of greater foundation distance (for k_h = 0.1). But, when k_h = 0.4, location of such a pile remains unchanged, and the more the foundation distance, the higher the maximum seismic bearing capacity. The maximum seismic bearing capacity increases by 35% for low horizontal seismic coefficient, in case S increases from 0 to B (Figure 7a). Also, the maximum seismic bearing capacity increases by 115% for high horizontal seismic coefficient (Figure 7b). In fact, the effect of foundation distance on seismic bearing capacity depends mainly on the horizontal seismic coefficient. Results show that when k_h = 0.1, the location of this kind of pile changes from slope crest to L_x/L = 0.65 as a result of any increase in foundation distance to B; however, when k_h = 0.4, its location is close to the slope crest at various foundation distances, relative to the slope crest, itself.

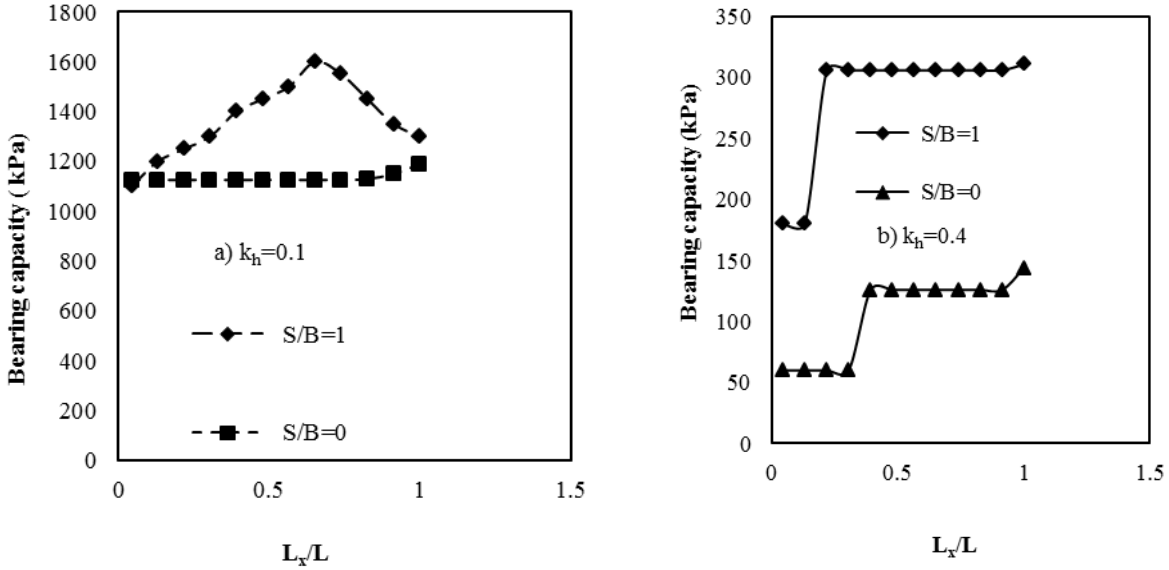

Fig. 7. Effect of footing distance, relative to slope crest on footing seismic bearing capacity for various locations of pile in slope: (a) k_h = 0.1, and (b) k_h = 0.4

In general, when k_h = 0.1 and the footing is located near slope crest, the footing seismic bearing capacity from virtual retaining wall method is minimum in all locations of the pile in the slope. When the pile is installed near the lower half of the slope, an increase in seismic horizontal coefficient (k_h) up to 0, 4, results in minimum footing bearing capacity, using the seismic slope stability method. When the pile is installed in other parts of the slope, virtual retaining wall method gives minimum seismic bearing capacity. When k_h = 0.1 and foundation distance increases with respect to slope crest ($S = B$), seismic slope stability method gives minimum seismic bearing capacity in all locations of the pile in the slope. In fact, increasing foundation distance from the slope crest results in higher seismic bearing capacity using the virtual retaining wall method than by seismic slope stability method and, consequently, seismic slope stability method results in minimum seismic bearing capacity. But, when k_h = 0.4 and foundation distance relative to slope crest (S) increases in various parts of the pile in the slope, seismic bearing capacity that results in minimum value is determined with the same method, because as horizontal seismic coefficient increases, seismic bearing capacity, which employs both methods (i.e. slope stability and virtual retaining wall) decreases remarkably. Therefore, the method of seismic bearing capacity determination that results in minimum value does not vary as the foundation distance increases.

Effects of Foundation Depth

Figure 8a indicates that by increasing foundation depth from 0 to 0.5B, maximum seismic bearing capacity is achieved when the pile row moves from the slope crest to the middle of the slope (L_x/L = 0.65) for k_h = 0.1 (L_p/b = 20 , S/B = 0, B = 2 m). This is due to the change in determining method of the footing seismic bearing capacity from virtual retaining wall to seismic slope stability for most pile locations in the slope. When the pile row is installed in the middle of the slope, pile length in sliding surface increases and maximum footing seismic bearing capacity is then achieved. When k_h = 0.1, and D/B = 0.5, increasing foundation depth leads to higher passive force (Eq. 8), more footing seismic bearing capacity from virtual retaining wall method, as well as deeper foundation and minimum seismic bearing capacity from seismic slope stability method in most pile locations in the slope. Figure 8a also shows that when k_h = 0.1, increasing foundation depth to 0.5B results in a 75% increase in the footing seismic bearing capacity as a result of the fact that by increasing the foundation depth, the soil weight in the rupture surface decreases. Then, the seismic bearing capacity with seismic slope stability method increases.

When k_h = 0.4, varying footing depths do not affect pile location in the slope that results in maximum seismic bearing capacity, yet the effect of foundation depth on maximum footing seismic bearing capacity is remarkable (Figure 8b). This is because minimum footing seismic bearing capacity is obtained with virtual retaining wall method for almost all pile row locations in the slope. Based on these findings, when k_h = 0.4 and foundation depth increases up to 0.5B, the ratio of maximum seismic bearing capacity with a D = 0.5B foundation to maximum seismic bearing capacity with a D/B = 0 foundation is equal to 2.5. Therefore, the influence of foundation depth on seismic bearing capacity increases when seismic horizontal coefficient goes up. Results, shown in Figure 8b, indicate that by increasing horizontal seismic coefficient, foundation depth does not alter pile row location, leading to maximum footing seismic bearing capacity, which increases remarkably.

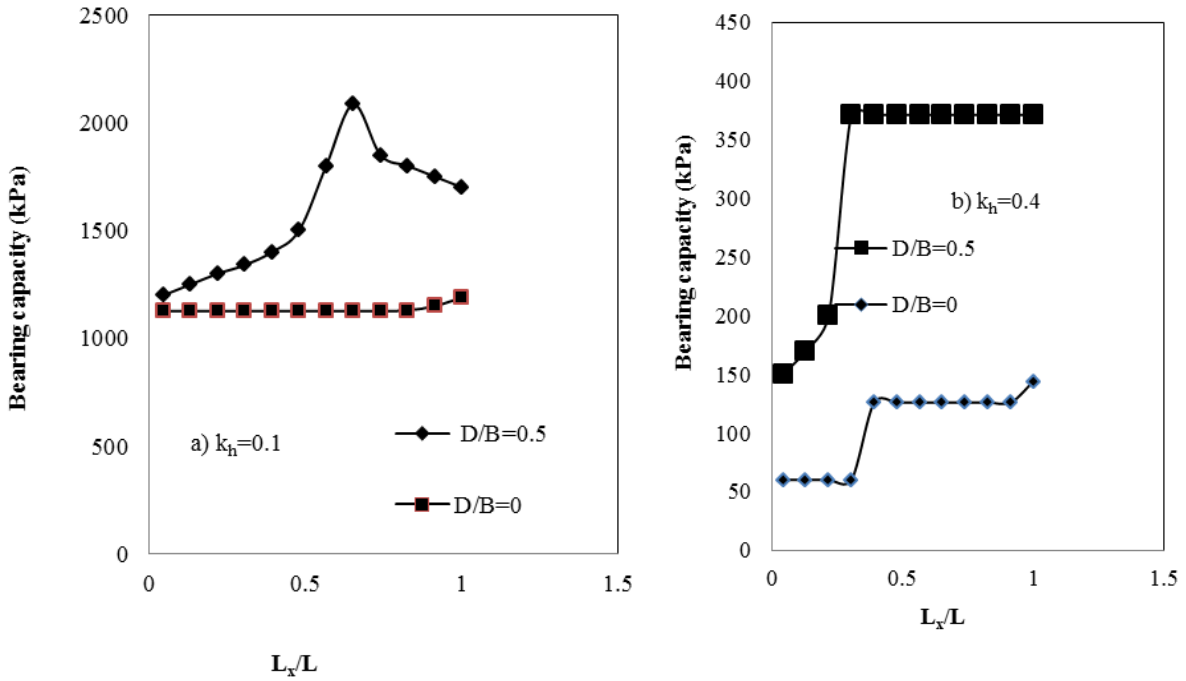

Fig. 8. Effect of foundation depth on footing seismic bearing capacity for various locations of pile in slope: (a) k_h = 0.1; and (b) k_h = 0.4

CONCLUSIONS

In the present study, the seismic bearing capacity of footing in a slope, reinforced with pile rows, has been investigated with two analytical solutions based on retaining wall and seismic slope stability methods. Comparisons show a reasonable compatibility between the results of the proposed method and those, reported by others. The following remarks may be cited from the results:

1. The effect of foundation distance, relative to slope crest on maximum seismic bearing capacity, and the location of the pile that results in maximum seismic bearing capacity depend on seismic horizontal coefficient. The latter is transferred from slope crest to L_x/L = 0.65 in low horizontal seismic coefficient (k_h = 0.1) when foundation distance increases with respect to slope crest (S = B), but as seismic horizontal coefficient and foundation distance increase, it does not vary and remains near slope crest. When foundation distance changes from 0 to B, the maximum seismic bearing capacity increases by 35% in low horizontal seismic (k_h = 0.1) and by 115% in high coefficient (k_h = 0.4).
2. When $D/B \geq 0.5$, foundation depth affects seismic bearing capacity and the location of the pile that results in maximum seismic bearing capacity. However, when $D/B < 0.5$, the effect of foundation depth on the maximum seismic bearing capacity and the location of such a pile is negligible for various horizontal seismic coefficients. By increasing foundation depth, location of this kind of pile is transferred from slope crest to L_x/L = 0.65 in low horizontal seismic coefficient (k_h = 0.1) and does not change as seismic horizontal coefficient increases. Also, foundation depth has more effect on maximum seismic

bearing capacity when an increase occurs in seismic horizontal coefficient.

ACKNOWLEDGEMENTS

The author's appreciation and acknowledgement goes for the support provided by the Islamic Azad University, Islamshahr Branch.

REFERENCES

Auslio, E., Conte, E. and Dente, G. (2001). "Stability analysis of slopes reinforced with piles", *Computers and Geotechnics*, 28(8), 591-611.

Azzam, W.R. (2010). "Experimental and numerical studies of sand slopes loaded with skirted strip footing", *Electronic Journal of Geotechnical Engineering*, 15(H), 795-812.

Chen, W.F. (1975). *Limit analysis and soil plasticity*, Elsevier Publishing Company, Amsterdam.

Choudhury, D. and Rao, S. (2006). "Seismic bearing capacity of Shallow strip footings Embedded in Slope", *International Journal of Geomechanics*, 6(3), 176-184.

Farzaneh, O., Askari, F. and Hadad, B. (2009). "Experimental modeling of three dimensional bearing capacity of footings on slopes", *Civil Engineering Infrastructures Journal*, 43(1), 85-93.

Hassiotist, S. and Chameau, J.L. (1997). "Design method for stabilization of slopes with piles", *Journal of Geotechnical and Geoenvironmental Engineering*, ASCE, 123(4), 314-322.

Hansen, J.B. (1970). "A revised and extended formula for bearing capacity", *Bulletin 28*, Copenhagen, Danish Geotechnical Institute.

Ito, T. and Matsui, T. (1975). "Methods to estimate lateral force acting on stabilizing piles", *Soils and Foundations*, 18(4), 43-59.

Liu, Y. and Geo, F. (2015). "Dynamic stability analysis on a slope supported by anchor bolts and piles", *Electronic Journal of Geotechnical Engineering*, 20(7), 1887-1900.

Mehmetl, M. (2009). "Determination of lateral loads on slope stabilizing piles", *Journal of Pamukkale Universitesi Miihendislik Bilimreli Dergisi*, 15(2), 194-202.

Meyerhof, G.G. (1963). "Some recent research on the bearing capacity of foundations", *Canadian Geotechnical Journal*, 1(1), 16-27.

Mofidi, J., Farzaneh, O. and Askari, F. (2014). "Bearing capacity of strip footings near slopes using lower bound limit analysis", *Civil Engineering Infrastructures Journal*, 47(1), 89-109.

Mostafa, A. and Sawwaf, E. (2005). "Strip footing behavior on pile and sheet pile-stabilized sand slope", *Journal of Geotechnical and Geoenvironmental Engineering*, ASCE, 131(6), 705-715.

Munawi, A., Murni Dewi, S., Agoes Soehardjono, M. and Zaika, Y. (2013). "Bearing capacity of continuous footing on slope modeling with composite bamboo pile reinforcement", *International Journal of Current Engineering and Technology*, 3(2), 557-562.

Munawir, A., Murni, D., Yulvi, Z. and Soehardjono, M. (2013). "Bearing capacity on slope modeling with composite bamboo pile reinforcement", *International Journal of Engineering and Advanced Technology (IJEAT)*, 2(5), 114-118.

Munawir, A., Murni Dewi, S. and Zaika, Y. (2013). "Safety factor of continuous footing on slope modeling with composite bamboo pile reinforcement", *Electronic Journal of Geotechnical Engineering*, 18(K), 2177-2186.

Ren-Ping, L. (2009). "Stability analysis of cutting slope reinforced with anti-slide piles by FEM", *GeoHunan International Conference*, Changsha, Hunan, China.

Saran, S., Sud, V.K. and Handa, S.C. (1989). "Bearing capacity of footings adjacent to slopes", *Journal of Geotechnical Engineering*, ASCE, 115(4), 553-562.

Wei, W.B. and Cheng, Y.M. (2009). "Strength reduction analysis for slope reinforced with one row of piles", *Computers and Geotechnics*, 36, 1176-1185.

Xinpo, L., Siming, H. and Yong, W. (2010). "Seismic displacement of slopes reinforced with piles", *Journal of Geotechnical and Geoenvironmental Engineering*, ASCE, 136(6), 1140-1155.

APPENDIX

$$f_1 = \frac{(3(\tan(\phi)/FS)\cos(\theta_h)+\sin(\theta_h))e^{3(\theta_h-\theta_0)\frac{\tan(\phi)}{FS})} - 3\tan(\phi)\cos(\theta_0)-\sin(\theta_0)}{3(1+9(\tan^2(\phi)/FS^2))}$$

$$f_2 = \frac{1}{6}\frac{L_1}{r_0}(2\cos(\theta_0 - \frac{L_1}{r_0}\cos(\alpha))\sin(\theta_0+\alpha)$$

$$f_3 = \frac{e^{(\theta_h-\theta_0)\frac{\tan(\phi)}{FS}}}{6}\left[\sin(\theta_h-\theta_0)-\frac{L_1}{r_0}\sin(\theta_h+\alpha)\right]\left\{\cos(\theta_0)-\frac{L_1}{r_0}\cos(\alpha)+\cos(\theta_h)e^{(\theta_h-\theta_0)\frac{\tan(\phi)}{FS}}\right\}$$

$$f_4 = \left[\frac{H}{r_0}\right]^2 \frac{\sin(\beta-\beta')}{2\sin(\beta)\sin(\beta')}\left[\cos(\theta_0)-\frac{L_1}{r_0}\cos(\alpha)-\frac{H}{3r_0}\left[\cot(\beta)-\cot(\beta')\right]\right]$$

$$f_5 = \frac{(3\tan(\phi)/FS)\sin(\theta_h)-\cos(\theta_h))e^{3(\theta_h-\theta_0)\frac{\tan(\phi)}{FS}} - 3(\tan(\phi)/FS)\sin(\theta_0)+\cos(\theta_0)}{3(1+9(\tan^2(\phi)/FS^2))}$$

$$f_6 = \frac{L_1}{6r_0}(2\sin(\theta_0)+\frac{L_1}{r_0}\sin(\alpha))\sin(\theta_0+\alpha)$$

$$f_7 = \frac{e^{(\theta_h-\theta_0)\frac{\tan(\phi)}{FS}}}{6}\left[\frac{H}{r_0}\right]\frac{\sin(\theta_h+\beta')}{\sin(\beta')}\left[2\sin(\theta_h)e^{(\theta_h-\theta_0)\frac{\tan(\phi)}{FS}} - \left[\frac{H}{r_0}\right]\right]$$

$$f_8 = \left[\frac{H}{r_0}\right]^2 \frac{\sin(\beta-\beta')}{6\sin(\beta)\sin(\beta')}\left[3\sin(\theta_h)e^{(\theta_h-\theta_0)\frac{\tan(\phi)}{FS}} - \frac{H}{r_0}\right]$$

$$f_9 = \frac{1}{2\tan(\phi)}\left\{e^{2(\theta_h-\theta_0)\frac{\tan(\phi)}{FS}} - 1\right\}$$